[1.] Corina Daniela CUNȚAN, [2.]Gabriel Nicolae POPA, [3.]Corina Maria DINIŞ, [4.] Angela IAGĂR

ANALYSIS OF LC PASSIVE FILTERS USED FOR SINGLE–PHASE WELDING MACHINE

[1–4.]Politehnica University of Timisoara, Faculty of Engineering Hunedoara, Hunedoara, ROMANIA

Abstract: Harmonics is the most important dynamic component of power quality, which affects the operation of electrical devices while reducing the power factor. Switched mode power sources in energy systems are generally associated with nonlinear loads. In this paper was analyzed a nonlinear single–phase consumer consisting of a manual welding machine of the XENTA 90 type, without passive filters and equipped with LC passive filters. In order to analyze the operation of LC passive filters, seven experiments were conducted. For consumers, attenuation of current waveform distortion depends on the values of L, C and, especially depends on the ability to improve the power factor to increase the efficiency of passive filters. With appropriate choice of passive LC filters, the deformation rate decreases and the electrical losses of the network are reduced by increasing the power factor.
Keywords: LC passive filters, welding machine, power factor, harmonics, THD

1. INTRODUCTION

Energy consumption and power quality are closely related both in industrial and non–industrial applications. Power factor and total harmonic distortion are two crucial indicators of power quality that correlate with the efficiency of electricity for both electricity suppliers and consumers [1–3].
Because of their low cost and efficiency, passive power filters (PPFs) are, usually, used to suppress harmonics and improve the power factor by tuned LC and/or low–pass filters [4–11]. However, PPFs have the following disadvantages: the source impedance and their operation in transitory regimes have a significant impact on filter quality; the parallel resonance between the source and the PPF increases the harmonic current at a given frequency on the source side [12,13].
If power quality indices differ from the compatibility standard, this results in significant implications for producers, system operators, and energy consumers. Poor power quality is associated with reduced productivity, equipment breakdown, significant financial losses, and shorter life expectancy of electrical system components and final applications. Electromagnetic disturbances that occur during the operation of energy systems affect almost all characteristics of voltage and current waves: frequency, shape, amplitude and symmetry (in the case of three–phase systems) [14,15].
Harmonics are the most important and dynamic component of electromagnetic disturbances. Harmonic sources in energy systems are typically associated with nonlinear and switching loads (e.g., rectifiers, inverters, voltage controllers, frequency converters, welding, AC or DC motor drives, switching power supply, fluorescent lamps and LED lamps, static VAR compensators, etc.). In recent years, power networks have been exposed to various harmonic sources, which have a direct impact on the sustainability of power plants such as wind and solar power stations, direct current conversion and high voltage transmission, etc. [2]

2. INVERTER TYPE WELDING DEVICES

Figure 1 shows a block diagram of a power source with an inverter. The main rectifier is an uncontrolled bridge–type rectifier of single or three phases (depending on the power installed and the range of power output current). The rectifier's power supply circuit is connected by a varistor to protect against accidental overvoltages from the power supply. In the modern version of the reversible power source, the input rectifier is equipped with an active filter to improve the power factor (PFC – Power Factor Correction).

ISSN 1584 – 2665 (printed version); ISSN 2601 – 2332 (online); ISSN-L 1584 – 2665

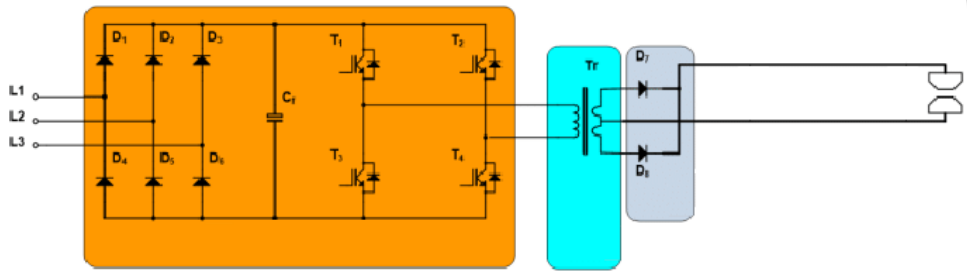

Figure 1. Inverter welding power source.

The intermediate DC filter is a capacitance type that has the role of reducing the reversal voltage vibration applied to the inverter. The capacitor is an electrolytic type with appropriate nominal voltage and low dielectric losses. For the first charge of the capacitor on the connection, in general an additional resistor circuit is provided, which is then short–circuited by a contact of an auxiliary relay [16].

The primary inverter block is the primary switch block (high frequency electronic switch) implemented with different types of power semiconductor devices, in different topological configurations (forward, half bridge, and bridge). According to the type of power semiconductor device, circuit topology, and specific output power control requirements, inverter block control is performed through various pulse width modulation strategies (PWM – pulse width modulation).

The high frequency adjustment transformer is a magnetic component that connects the circuit (welding with the supply power) and ensures the operator's electrical safety and voltage adaptation. The construction of the transformer is dictated by considerations aimed at minimizing power loss and dispersion inductance, and is composed of ferrite cores of different shapes, or windings of wire or copper foil type, respectively, to reduce additional losses due to eddy currents [16].

The high frequency secondary rectifier has the role of rectifying the high frequency alternating voltage to supply the direct current welding arc. It is made of super–fast rectifier diodes, in different configurations (with median point or single–phase bridge). The output filter is inductive type and has the role of reducing changes in continuous welding current and, respectively, ensuring a rapid reaction. Because of the high working frequency, the input value is low (μH), and the input of connecting conductors associated with welding circuits also contributes to smoothing current.

3. EXPERIMENTAL RESULTS OBTAINED WITH THE CA8334B POWER QUALITY ANALYZER

The circuit from Fig.2.a was used to carry out the experimental measurements (Fig.2.b), in order to determine the impact of welding machine on power network.

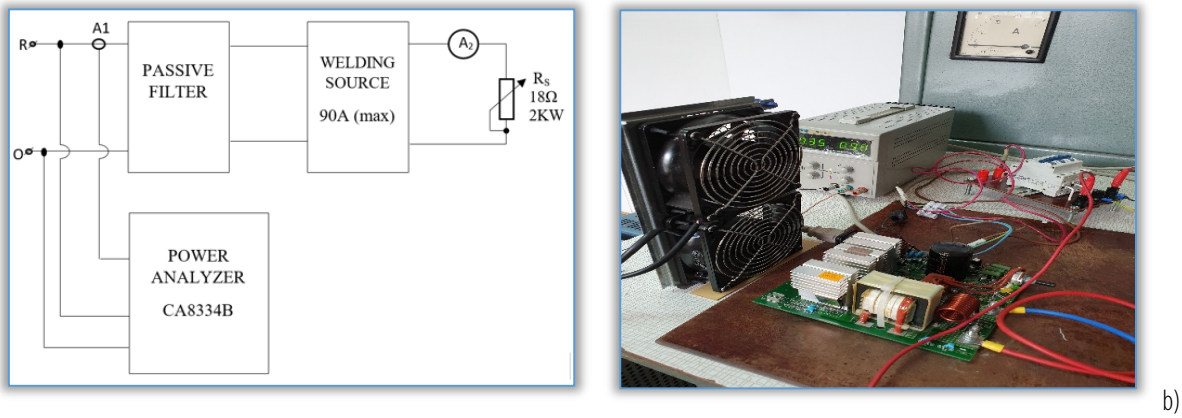

a) b)

Figure 2. a) Block diagram of the studied circuit; b) experimental setup.

Measurement results when the welding machine (which has a resistive load) is not equipped with a passive filter

The measurements with power quality analyzer CA8334B on the welding machine with a resistive load of 18 Ω/2 kW, show that a very high–value of current harmonic distortion factor THD_I is reduced once with the increase in welding current (I is the input AC current; Is is the output DC current) and

ISSN 1584 – 2665 (printed version); ISSN 2601 – 2332 (online); ISSN-L 1584 – 2665

implicitly with the current absorbed from the network (Fig.3.a). A relatively low value for the power factor (PF) is found, slightly above 0.66; PF remains approximately constant when welding current have significant changes (Fig.3.c). At the same time, displacement power factor (DPF) has a small variation when welding current changes; DPF has an inverse variation in relation to the PF with increased output current (Table 1). In all situations, higher values of reactive power than active power values can be observed (Table 1).

Table 1 – Experimental measurements of resistive load welding device ($R_L = 1.5\ \Omega$) without passive filters

I(A)	THD_I(%)	P(W)	Q(VAR)	S(VA)	PF(–)	DPF(–)	I_s(A)
2.4	105.2	364	410.5	550.3	0.662	0.988	9
3.8	104.5	573.2	655.4	872.4	0.659	0.98	16
5.6	103	827	940	1249	0.66	0.972	23
7.1	98.9	1056	1174	1578	0.67	0.965	30
8.7	95.2	1297	1413	1920	0.676	0.959	37
9.3	93.2	1403	1501	2056	0.683	0.957	42

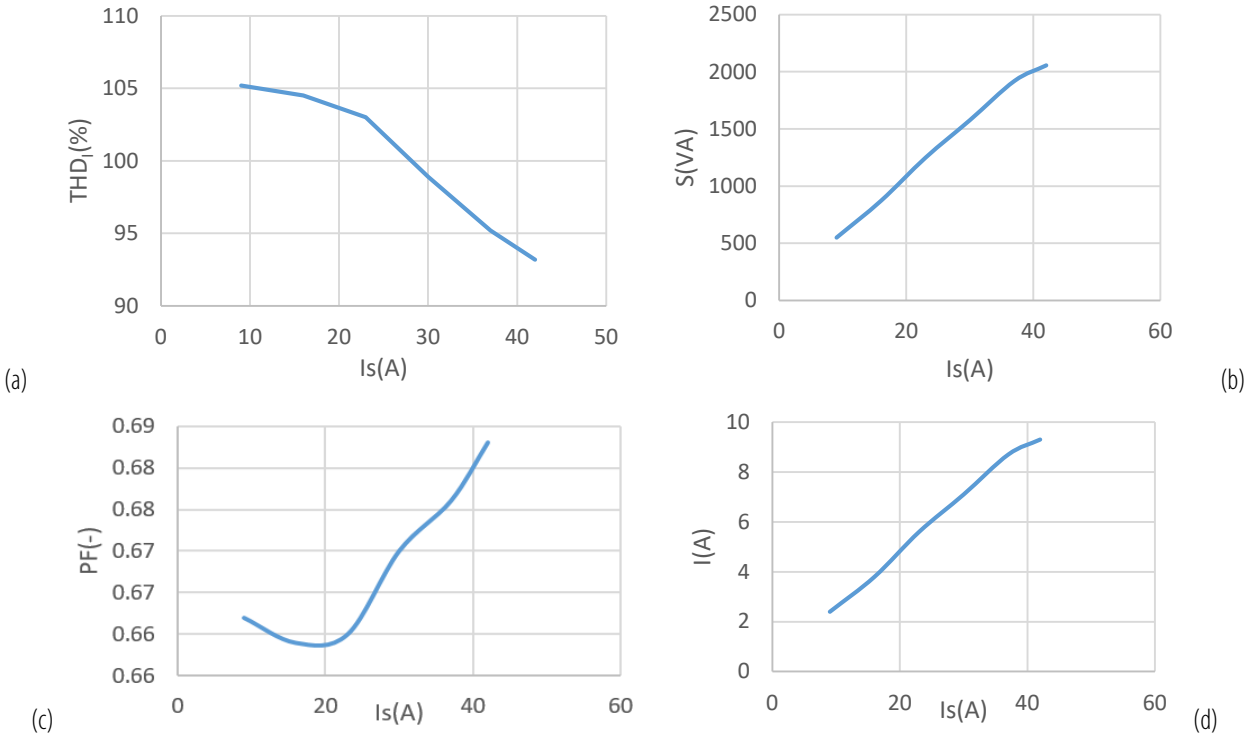

Figure 3. Measurement results: a) $THD_I = f(I_s)$; b) $S = f(I_s)$; c) $PF = f(I_s)$; d) $I = f(I_s)$

Figure 4.a presents the waveforms of voltage and current over a period; it can be observed that voltage have a shape close to sinusoidal (RMS value was 225 V), but the waveform of current is very deformed (RMS value was 2.4 A (Fig.4.a). This can also be seen from the spectrum of current harmonics, that have the most important values for lower orders, and total harmonic distortion factor THD_I has more than 100%. Figure 4.c shows a relatively low phase shift of 9° between voltage and current (for the fundamental).

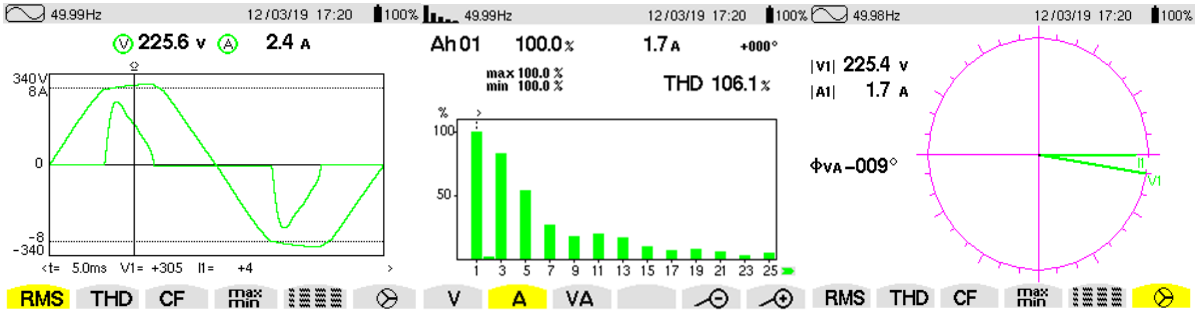

Figure 4. Measurements with CA 8334B: a) voltage and current waveforms over a period;
b) harmonic spectrum and total harmonic distortion factor (THD_I) for current; c) Fresnel diagram for the fundamental at $I_s = 9$ A

ISSN 1584 – 2665 (printed version); ISSN 2601 – 2332 (online); ISSN-L 1584 – 2665

The measurement results obtained at a current of 30 A (Fig.5) show the same behavior of the welding machine as with a current of 9 A; an increase in the phase shift of 15° it observed.

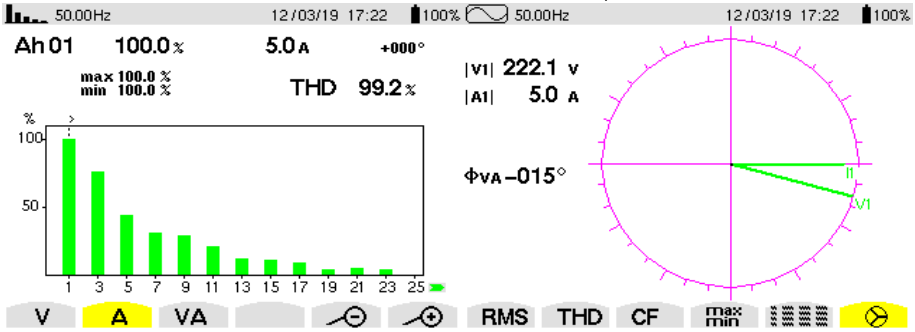

Figure 5. Measurements with CA 8334B: a) harmonic spectrum and total harmonic distortion factor (THD_I) for current; b) Fresnel diagram for the fundamental at I_s= 30 A

- Results of measurements made when the welding machine (having resistive load) was connected with L filter (Fig.6)
  - First L filter (L=9.86 mH)

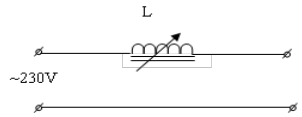

Figure 6. L filter connected in circuit.

In this situation, total harmonic distortion factor for current THD_I have much lower values compared to the previously situation, but still high, over 50%. A significant increase in the power factor (PF), over 0.8, and the displacement power factor (DPF) of over 0.95 is also observed (Table 2).

Table 2 – Experimental measurements made with the resistive load welding device (R_L = 1.5 Ω) and the first inductive filter (L = 9.86 mH)

I(A)	THD_I(%)	P(W)	Q(VAR)	S(VA)	PF(–)	DPF(–)	I_s(A)
1.9	76	335.3	278	435.6	0.769	0.967	9
3.2	67.1	559.5	425.7	701.9	0.796	0.961	16
4.4	60.8	798.5	565.9	977.8	0.816	0.957	23
5.7	55.7	1053	708	1268	0.829	0.953	30
6.7	52.3	1230	805	1477	0.837	0.95	37
6.9	51.9	1264	823	1508	0.838	0.949	42

In this case, the active power is significantly higher than the reactive power. The variation of the current is closer to a sinusoidal shape than in previously case, and the values of higher–order harmonics are reduced while those of lower–order harmonics remain high. The phase shift between voltage and current (for the fundamental) is relatively small and has the opposite value compared to the previous case (Table 2, Figs.7–9).

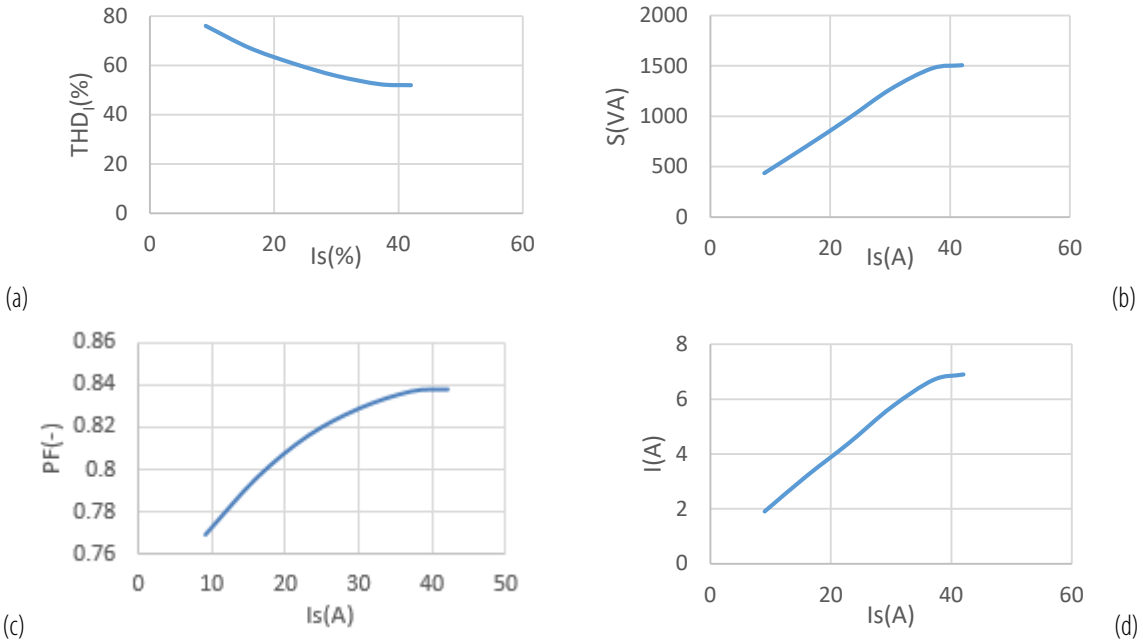

Figure 7. Measurement results: a) THD_I=f(I_s); b) S=f(I_s); c) PF=f(I_s); d) I=f(I_s).

ISSN 1584 – 2665 (printed version); ISSN 2601 – 2332 (online); ISSN-L 1584 – 2665

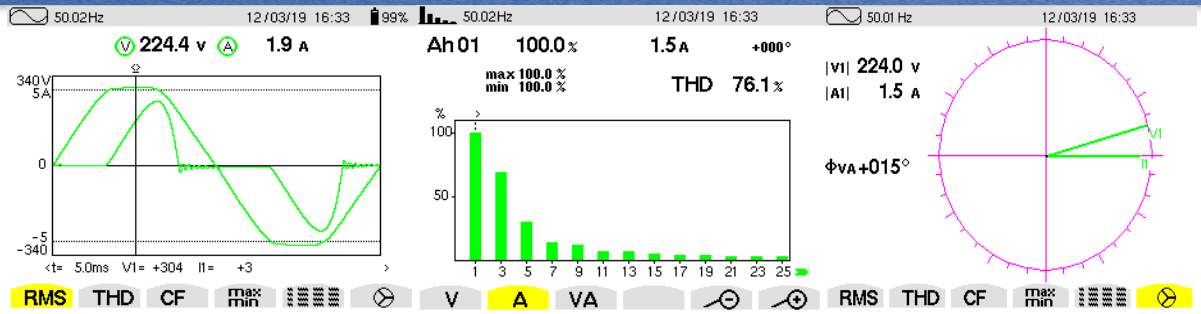

Figure 8. Measurements with CA 8334B: a) voltage and current waveforms over a period;
b) harmonic spectrum and total harmonic distortion factor (THD_I) for current; c) Fresnel diagram for the fundamental at I_s= 9 A

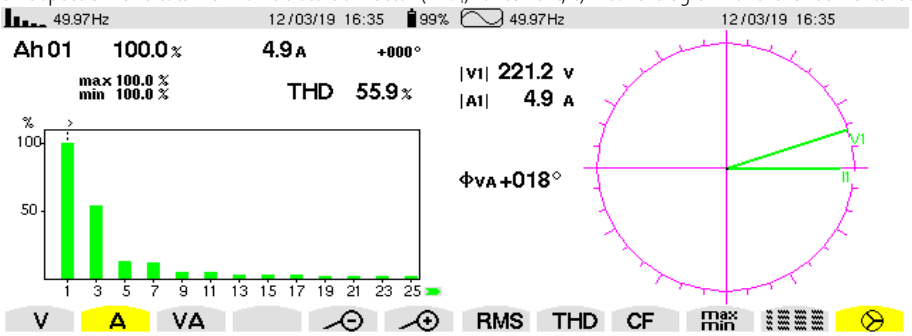

Figure 9. Measurements with CA 8334B: a) harmonic spectrum and total harmonic distortion factor (THD_I) for current; b) Fresnel diagram for the fundamental at I_s= 30 A

— Second L filter (L=23.7 mH)

The increase in the value of the filtering inductance further reduces the THD_I factor, with lower values at higher output currents; an increase in the share of active power at the expense of reactive power it is observed. At the same time, a higher power factor (PF) is achieved, with higher values at higher currents, while the displacement power factor (DPF) varies inversely, meaning that at higher currents, a lower value is obtained.

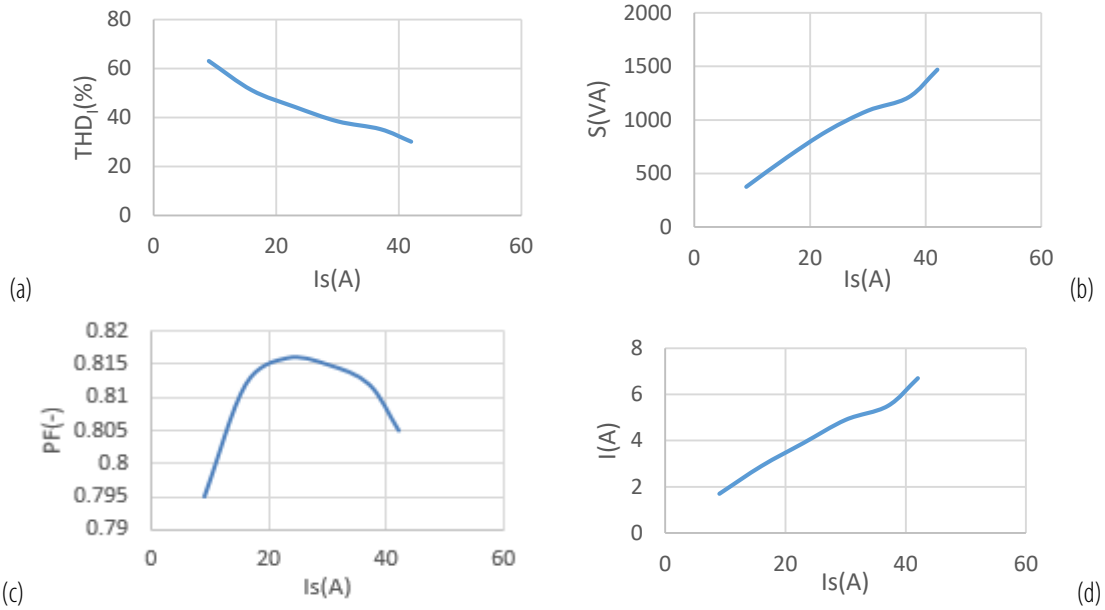

Figure 10. Measurement results: a) THD_I=f(I_s); b) S=f(I_s); c) PF=f(I_s); d) I=f(I_s).

Table 3 – Experimental measurements made with the resistive load welding device (R_L = 1.5 Ω) and the second inductive filter (L = 23.7 mH)

I(A)	THD_I(%)	P(W)	Q(VAR)	S(VA)	PF(–)	DPF(–)	Is(A)
1.7	63	299.1	228.5	375.5	0.795	0.937	9
2.9	51.1	526.3	378.6	649.5	0.812	0.913	16
3.9	44.3	710	502.2	897.4	0.816	0.894	23
4.9	38.4	885	629	1087	0.815	0.877	30
5.5	35.2	986	710	1211	0.812	0.865	37
6.7	30.1	1182	873	1470	0.805	0.844	42

ISSN 1584 – 2665 (printed version); ISSN 2601 – 2332 (online); ISSN-L 1584 – 2665

The analysis of Figs. 11 and 12 reveals a waveform of current closer to the sine wave; the harmonic values are reduced except for those of lower order. The phase shift remains at relatively low values, lower at lower currents (Table 3, Figs.10–12).

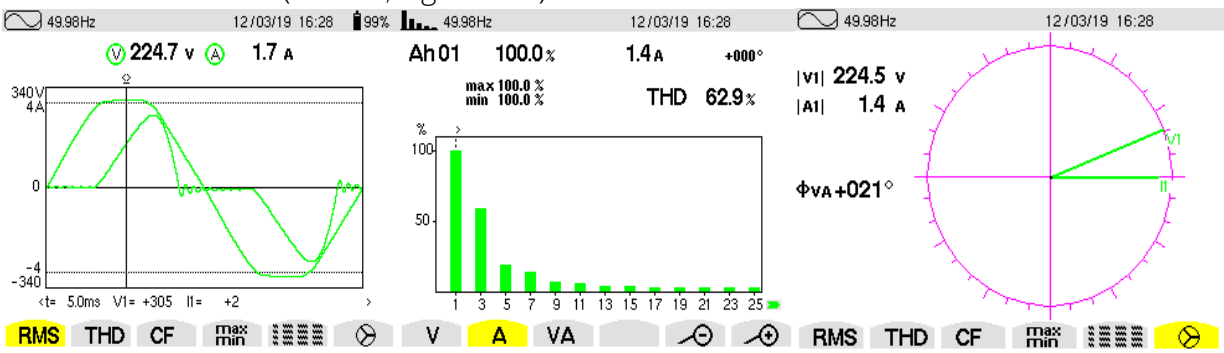

Figure 11. Measurements with CA 8334B: a) voltage and current waveforms over a period; b) harmonic spectrum and total harmonic distortion factor (THD_I) for current; c) Fresnel diagram for the fundamental at I_s= 9 A

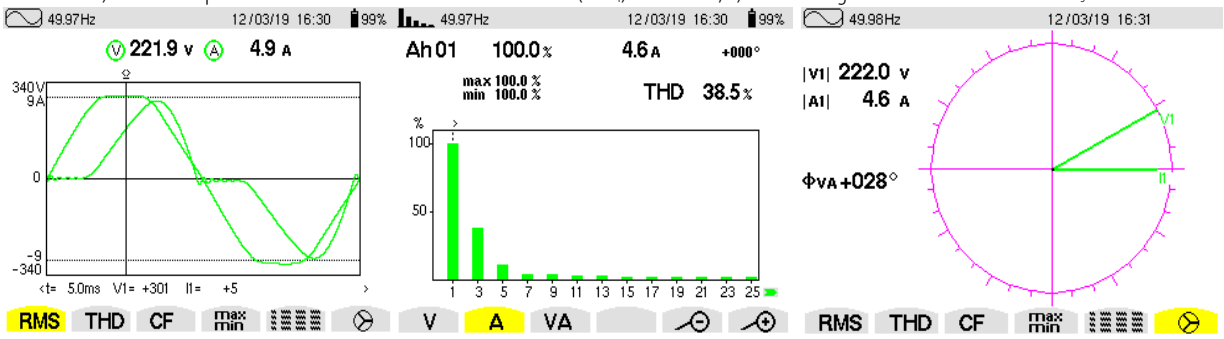

Figure 12. Measurements with CA 8334B: a) voltage and current waveforms over a period; b) harmonic spectrum and total harmonic distortion factor (THD_I) for current; c) Fresnel diagram for the fundamental at I_s= 30 A

- **Results of measurements made when the welding machine (having resistive load) was connected with LC filter (first layout, Fig.13)**

A variable inductance coil was used, $L = 9.1 \div 296\ mH$. Measurements were taken for two values of LC filter from Fig.13.

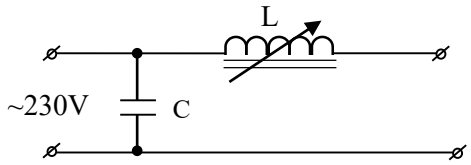

Figure 13. LC filter – first layout

— First LC filter (Fig.13, L = 9.86 mH, C = 10 μF)

Experimental measurements made with the resistive load welding device (R_L = 1.5 Ω) and the first LC filter (Fig.13, L = 9.86 mH, C= 10 μF) are present in Table 4 and Figs.14–16. It is observed that total harmonic distortion factor of current (THD_I) is over 50%, and decrease with the increase in welding current. The share of active power far exceeds that of reactive power, the power factor (PF) exceeds the value of 0.8, and the displacement power factor (DPF) tends towards unity. The values of the current harmonics are again significantly increased, the shape of the current has deviated from the sinusoid (Fig.15, 16), and the phase shift changes sign, meaning that at low current it is negative and at higher current it is positive.

Table 4 – Experimental measurements made with the resistive load welding device (R_L = 1.5 Ω) and the first LC filter (Fig.13, L = 9.86 mH, C= 10 μF)

I(A)	THD_I(%)	P(W)	Q(VAR)	S(VA)	PF(–)	DPF(–)	Is(A)
1.9	78.4	330.2	273.2	429	0.771	0.982	9
3.1	69.7	559.8	395.3	687.2	0.817	1	16
4.3	63	791.6	519.5	947.6	0.836	0.993	23
5.5	58	1014	635	1195	0.847	0.986	30
6.5	54	1209	734	1417	0.856	0.979	37
7	50	1430	844	1667	0.863	0.972	42

ISSN 1584 – 2665 (printed version); ISSN 2601 – 2332 (online); ISSN-L 1584 – 2665

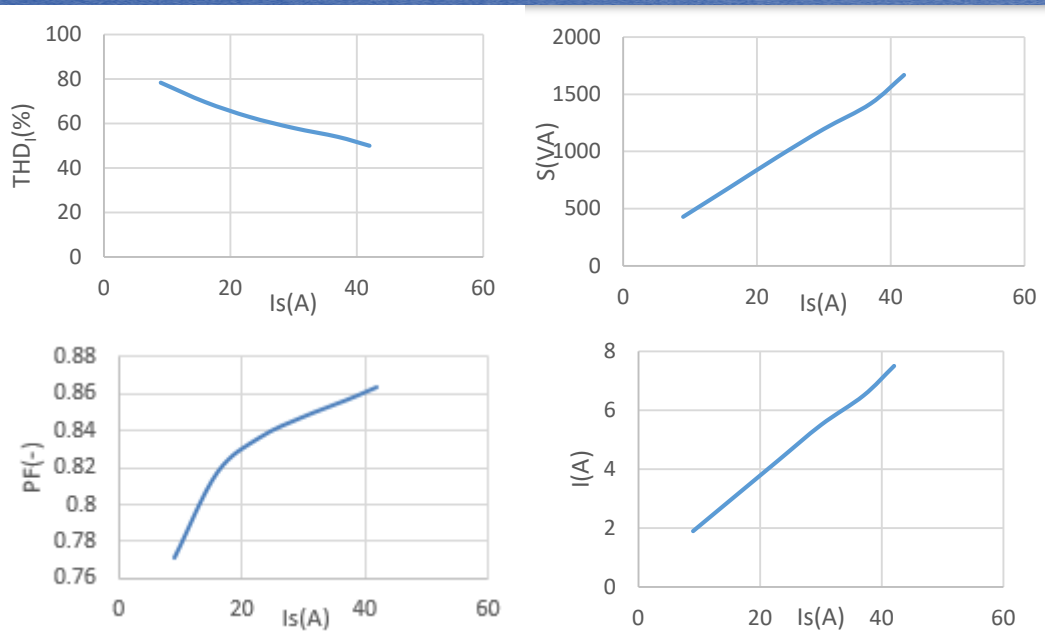

Figure 14. Measurement results: a) THD_I=f(Is) b) S=f(Is) c) PF=f(Is) d) I=f(Is)

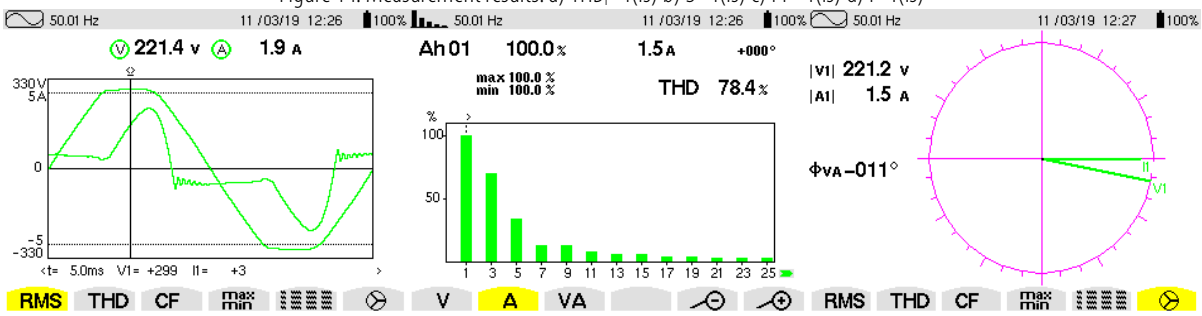

Figure 15. Measurements with CA 8334B: a) voltage and current waveforms over a period;
b) harmonic spectrum and total harmonic distortion factor (THD_I) for current; c) Fresnel diagram for the fundamental at I_s= 9 A

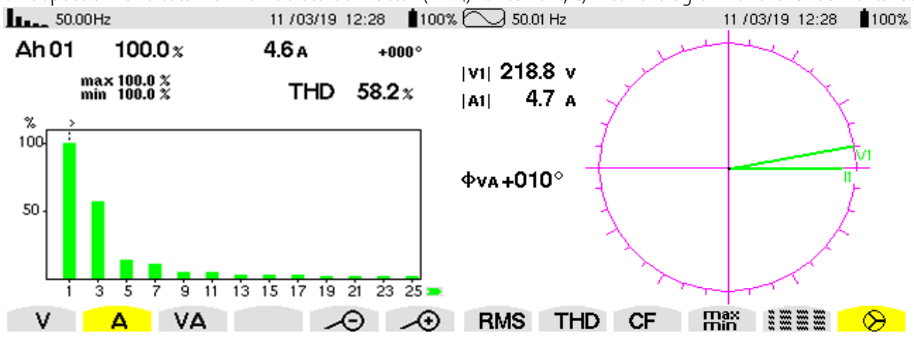

Figure 16. Measurements with CA 8334B: a) harmonic spectrum and total harmonic distortion factor (THD_I) for current; b) Fresnel diagram for the fundamental at I_s= 30 A

— Second LC filter (Fig.13, L=23.7 mH, C= 10 μF)

Table 5 – Experimental measurements made with the resistive load welding device (R_L = 1.5 Ω) and the second LC filter (Fig.13, L = 23.7 mH, C=10μF)

I(A)	THD_I(%)	P(W)	Q(VAR)	S(VA)	PF(–)	DPF(–)	I_S(A)
1.7	66.8	321.1	217.4	388.1	0.828	0.995	9
2.7	57	513.3	306	596.7	0.859	0.99	16
3.9	47.8	739	430	851.2	0.864	0.961	23
4.8	42.1	907	536	1052	0.861	0.937	30
5.7	37	1069	649	1250	0.854	0.914	37
6.5	33	1210	752	1425	0.849	0.898	42

In the case of second LC filter (Fig.13, L=23.7 mH, C= 10 μF) it is found that by increasing the inductance value of the filter, a lower THD_I factor up to 33% is achieved at a welding current of 42 A. The active power increased at the expense of the reactive power, and power factor (PF) exceeded 0.85, while displacement power factor (DPF) remained high, above 0.95.

ISSN 1584 – 2665 (printed version); ISSN 2601 – 2332 (online); ISSN-L 1584 – 2665

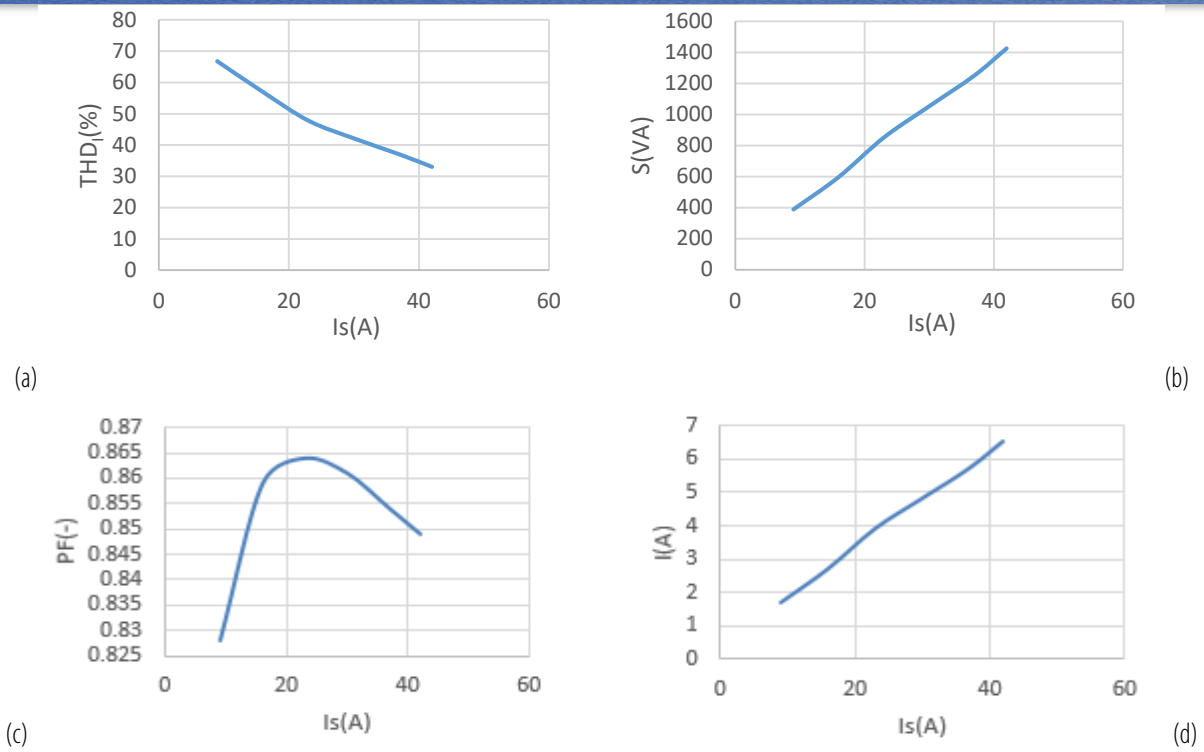

Figure 17. Measurement results: a) $THD_I=f(I_s)$; b) $S=f(I_s)$; c) $PF=f(I_s)$; d) $I=f(I_s)$.

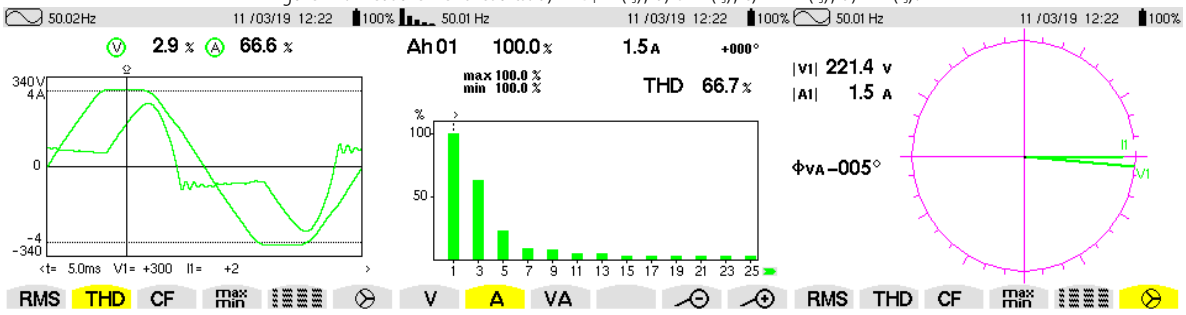

Figure 18. Measurements with CA 8334B: a) voltage and current waveforms over a period;
b) harmonic spectrum and total harmonic distortion factor (THD_I) for current; c) Fresnel diagram for the fundamental at I_s= 9 A

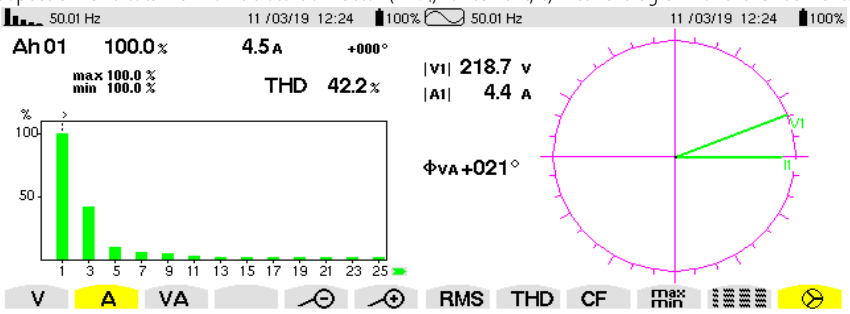

Figure 19. Measurements with CA 8334B: a) harmonic spectrum and total harmonic distortion factor (THD_I) for current; b) Fresnel diagram for the fundamental at I_s= 30 A

The values from Table 5 are reflected in Figs. 17–19. In this case the current waveform is closer to the sine wave, the high orders harmonics are reduced, and the phase shift remains negative at low current values and becomes positive with the increase in output current.

- **Results of measurements made when the welding machine (having resistive load) was connected with LC filter (second layout, Fig.20)**

The second layout of LC filter is presented in Fig. 20. In this case, the variable inductance coil (L=9.1÷296 mH) was placed towards the supply network. Measurements were taken for two values of this type of LC filter.

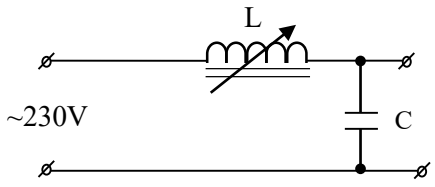

Figure 20. LC filter – second layout

ISSN 1584 – 2665 (printed version); ISSN 2601 – 2332 (online); ISSN-L 1584 – 2665

D1. Third LC filter (Fig.20, L=9.86 mH, C= 10 μF)

Table 6 and Figs.21–23 present the experimental measurements in the case of resistive load (R_L = 1.5 Ω) welding device and the third LC filter (Fig.20, L=9.86 mH, C= 10 μF). THD_I values continued to be higher, over 60%, depending on the output current; power factor (PF) varied around 0.8, and displacement power factor (DPF) was close to 1. The current distortion and its harmonic values are presented in Figs. 21–23; it is found a negative phase shift at low currents and a positive phase shift at higher currents (Fig.22.c, Fig.23.c).

Table 6 – Experimental measurements made with the resistive load welding device (R_L = 1.5 Ω) and the third LC filter (L = 9.86 mH, C=10 μF)

I(A)	THD_I(%)	P(W)	Q(VAR)	S(VA)	PF(–)	DPF(–)	I_S(A)
2.1	90	336.6	325.7	468.1	0.719	0.972	9
3.1	76.6	540.8	420.9	685.8	0.789	0.998	16
4.3	68.8	780.1	546.5	953	0.82	0.999	23
5.6	64.1	1002	674	1210	0.83	0.992	30
6.7	60.7	1242	832	1494	0.831	0.981	37
7.7	57.9	1422	947	1700	0.832	0.972	42

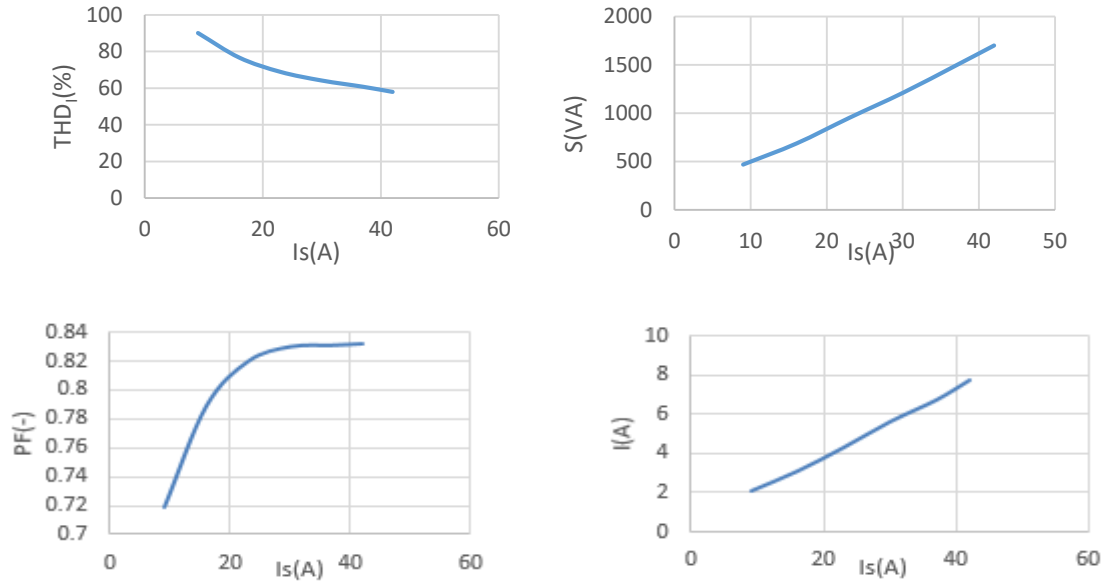

Figure 21. Measurement results: a) THD_I=f(I_S); b) S=f(I_S); c) PF=f(I_S); d) I=f(I_S).

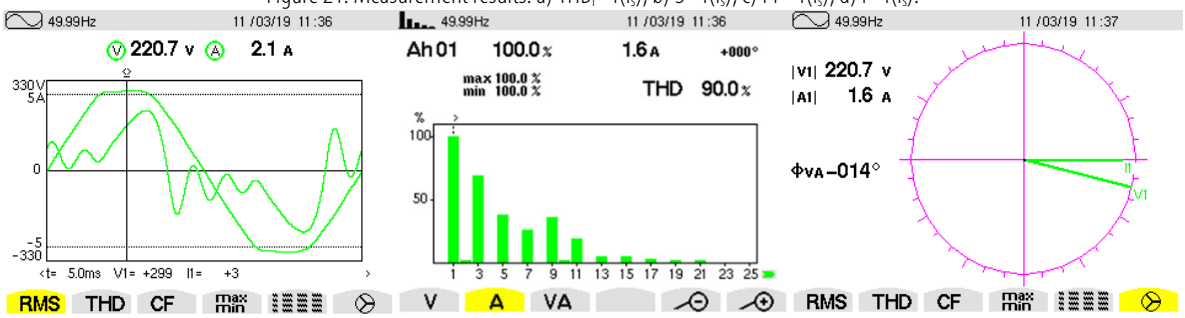

Figure 22. Measurements with CA 8334B: a) voltage and current waveforms over a period;
b) harmonic spectrum and total harmonic distortion factor (THD_I) for current; c) Fresnel diagram for the fundamental at I_S= 9 A

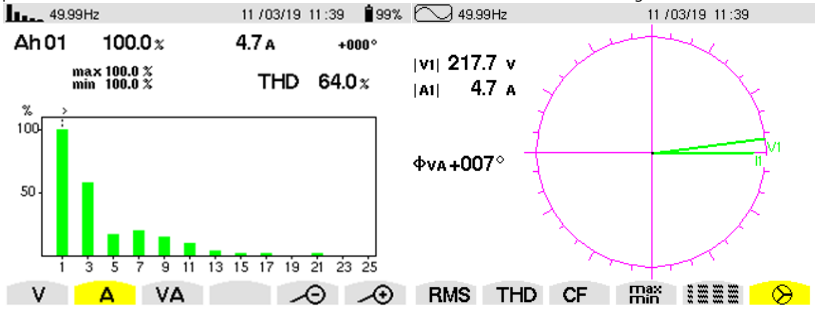

Figure 23. Measurements with CA 8334B: a) harmonic spectrum and total harmonic distortion factor (THD_I) for current; b) Fresnel diagram for the fundamental at I_S= 30 A

ISSN 1584 – 2665 (printed version); ISSN 2601 – 2332 (online); ISSN-L 1584 – 2665

Fourth LC filter (Fig.21, L=23.7 mH, C= 10 μF)

Table 7 and Figs.24–26 present the experimental measurements in the case of resistive load (R_L = 1.5 Ω) welding device and the fourth LC filter (Fig.21, L=23.7 mH, C= 10 μF).

With the increase of filter inductance to the value L=23.7 mH, a reduction in the total harmonic distortion factor of current (THD_I) is observed, down to almost 40% for an output current of 42 A. Additionally, it can be observed that the active power increases at the expense of reactive power, the power factor (PF) rises above 0.85 and the displacement factor (DPF) is maintained at values close to 1 (Figs.24–26).

Table 7 – Experimental measurements made with the resistive load–welding device (R_L = 1.5 Ω) and the fourth LC filter (L = 23.7 mH, C=10 μF)

I(A)	THD_I(%)	P(W)	Q(VAR)	S(VA)	PF(–)	DPF(–)	I_S(A)
2	77.1	332.7	279.3	434.8	0.766	0.966	9
3.1	65.9	557	367.8	667.8	0.834	1	16
4.2	60.2	773.5	500.1	922	0.840	0.983	23
5.2	56.8	920	645	1123	0.818	0.949	30
6	44.5	1155	690	1346	0.859	0.946	37
6.5	41.3	1223	696	1408	0.869	0.946	42

The data presented in Table 7 are consistent with the data from Fig.25, where the current waveform is more sinusoidal, and harmonic values are reduced with the exception of those of lower order. It is found a negative phase shift at low currents and a positive phase shift at higher currents (Fig.25.c, Fig.26.b).

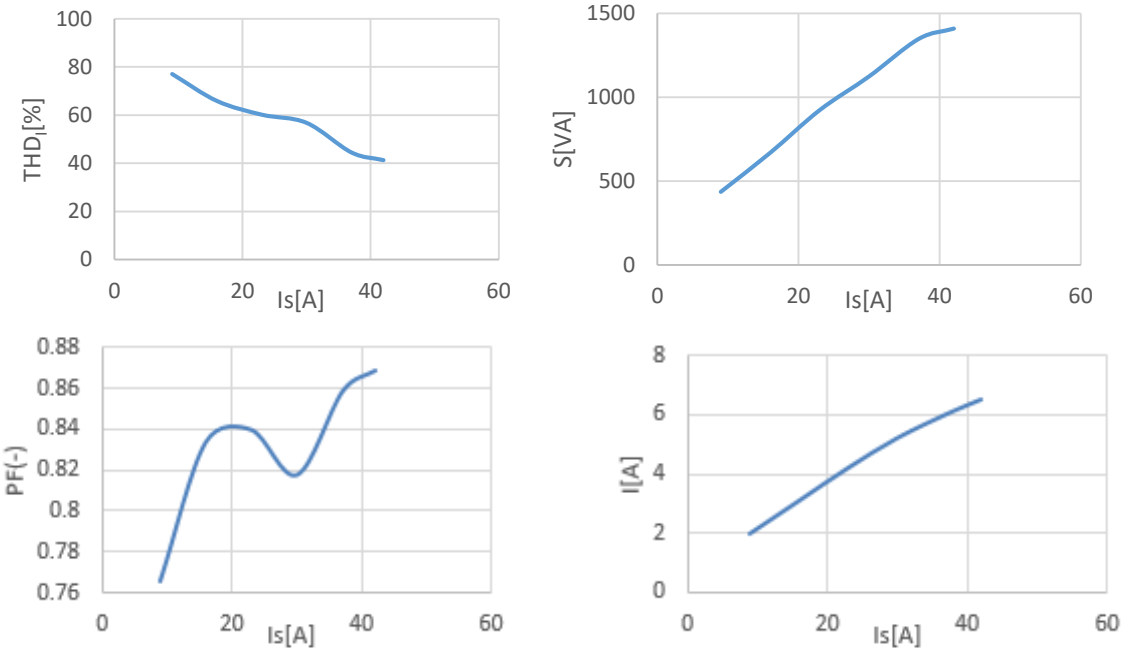

Figure 24. Measurement results: a) THD_I=f(I_s); b) S=f(I_s); c) PF=f(I_s); d) I=f(I_s).

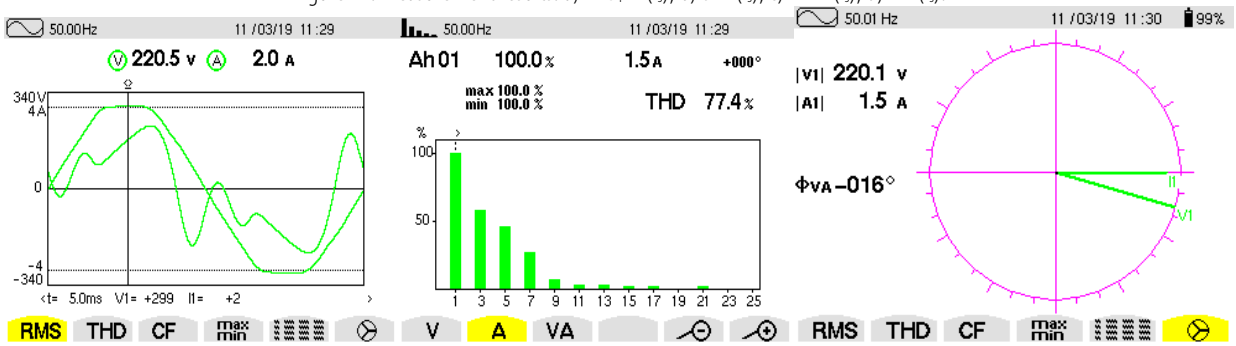

Figure 25. Measurements with CA 8334B: a) voltage and current waveforms over a period;
b) harmonic spectrum and total harmonic distortion factor (THD_I) for current; c) Fresnel diagram for the fundamental at I_s= 9 A

ISSN 1584 – 2665 (printed version); ISSN 2601 – 2332 (online); ISSN-L 1584 – 2665

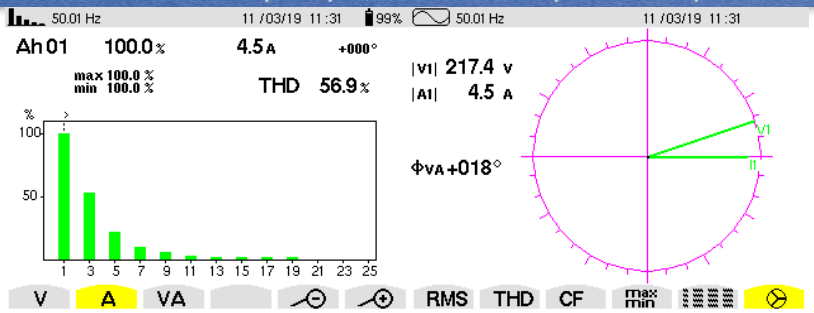

Figure 26. Measurements with CA 8334B: a) harmonic spectrum and total harmonic distortion factor (THDI) for current; b) Fresnel diagram for the fundamental at I_s= 30 A

4. CONCLUSIONS

In the experimental analysis of passive LC filters, a nonlinear consumer, commonly found in practice, a single–phase manual welding machine type XENTA 90 was used.

In the case of inductive filters, the best situation regarding harmonic distortion of current was obtained for the second L filter, where the coil inductance was higher. In this situation, total harmonic distortion factor of current varied between 30.1% and 63%. An increase in power factor values (over 0.8) and displacement power factor values (over 0.95) is also observed compared to the situation when the welding machine was not equipped with passive filters.

Experiments have shown that LC filters are more efficient in the first arrangement (layout). The best results in terms of harmonic filtering, but also in terms of power factor improvement, were obtained with the second LC filter. In this situation, total harmonic distortion factor of current varied between 33% and 66.8%. A significant increase in the power factor values (between 0.828 and 0.849) is achieved, compared to inductive filters.

Compared to the situation in which no filter is used, active power increases slightly by using LC passive filters, but displacement power factor decreases considerably, especially when using large filter capacities.

It is difficult to calibrate the LC passive filters to a certain harmonic, and it is almost impossible to adjust them.

At the same time, source impedance influences filter performance. When using LC passive filters, the network's AC current can increase by 5 percent compared to the situation without passive filters.

For this type of consumer the level of harmonic currents decreases as the order of the harmonics increases. The best filtering is performed with adjusted filters near the harmonic of order 3 to 5, but filters over this value are no longer as effective.

References

[1] Power Quality Application Guide. Available online: https://www.sier.ro/ghid_aplicare.html
[2] A.A. El–Ela, S.M. Allam, A.A. Mubarak, R.A. El–Sehiemy, "Harmonic Mitigation by Optimal Allocation of Tuned Passive Filter in Distribution System," Energy Power Eng. 2022, 14, 291–312.
[3] R.S. Widagdo, A.H. Andriawan, R. Hartayu, "Harmonic Mitigation in Microgrids to Improve Power Quality" J. Teknol. Elektro 2024, 15, 11–19.
[4] A.A. Abou El–Ela , S. Allam , H. El–Arwash "An Optimal Design Of Single Tuned Filter In Distribution Systems I" Electric Power Systems Research 78 (2008) 967–974.
[5] T.M.T. Thentral, S. Usha, R. Palanisamy, A. Geetha, A.M. Alkhudaydi, N.K. Sharma, M. Bajaj, S.S.M. Ghoneim, M. Shouran, S. Kamel, "An energy efficient modified passive power filter for power quality enhancement in electric drives" Front. Energy Res. 2022, 10, 1–20.
[6] R. Sirjani, B. Hassanpou" A New Ant Colony–Based Method for Optimal Capacitor Placement and Sizing in Distribution Systems" Research Journal of Applied Sciences, Engineering and Technology 4(8): 888–891, 2012.
[7] S.A. Sahidaini, "Electrical Power Quality Improvement through Modeling and Optimization of Passive Harmonic Filter" International Journal of Engineering Research & Technology (IJERT) ISSN: 2278–0181, Vol. 7 Issue 10, October–2018.
[8] O. A. Monem "Harmonic mitigation for power rectifier using passive filter combination" IOP Conf. Series: Materials Science and Engineering 610 (2019) 012013, IOP Publishing, doi:10.1088/1757–899X/610/1/012013.
[9] Z. A. Memon, M. A. Uquaili, A.M. A. Unar, "Harmonics Mitigation of Industrial Power System Using Passive Filters", Mehran University Research Journal of Engineering & Technology, Volume 31, No. 2, April, 2012 [ISSN 0254–7821].

[10] S.Rüstemli, E.Okuducu, M.N.Almali, S. B. Efe, "Reducing the effects of harmonics on the electrical power systems with passive filters" Bitlis Eren Univ J Sci & Technol 5 (1), 1 – 10, 2015.
[11] M. A. Soomro, A. A. Sahito, I. A. Halepoto, K. Kazi, "Single Tuned Harmonic Shunt Passive Filter Design for Suppressing Dominant Odd Order Harmonics in order to Improve Energy Efficiency" Indian Journal of Science and Technology, Vol 9(47), DOI: 10.17485/ijst/2016/v9i47/108649, December 2016.
[12] M.M. Ishaya, O.R. Adegboye, E.B. Agyekum, M.F. Elnaggar, M.M. Alrashed, S. Kamel, "Single–tuned passive filter (STPF) for mitigating harmonics in a 3–phase power system" Sci. Rep. 2023, 13, 20754.
[13] C.S. Azebaze Mboving, "Investigation on the Work Efficiency of the LC Passive Harmonic Filter Chosen Topologies" Electronics, 2021, 10, 896.
[14] G.N. Popa, A. Iagăr, C.M. Diniș, "Considerations on Current and Voltage Unbalance of Nonlinear Loads in Residential and Educational Sectors," Energies 2021, 14, 102.
[15] B. Park, J. Lee, H. Yoo, G. Jang, "Harmonic Mitigation Using Passive Harmonic Filters: Case Study in a Steel Mill Power System," Energies 2021, 14, 2278.
[16] T. Meng, H. Ben, Y. Song, C. Li,"Analysis and Design of an Input–Series Two–Transistor Forward Converter For High–Input Voltage Multiple–Output Applications" IEEE Transactions On Industrial Electronics, Vol. 65, No. 1, January 2018.

ISSN 1584 – 2665 (printed version); ISSN 2601 – 2332 (online); ISSN-L 1584 – 2665